Distribution of magnetic short-range order in spin-glasses

W. Kinzel and K. Binder
Institut für Festkörperforschung, Kernforschungsanlage Jülich D-5170 Jülich, Postfach 1913, West Germany
(Received 19 February 1981)

We discuss a description of the static magnetic order of spin-glasses at low temperatures in terms of the distribution function of spin-pair correlation functions, $P(g_{\vec{r}}) = P(\langle \vec{S}_{\vec{r}_1} \cdot \vec{S}_{\vec{r}_1+\vec{r}} \rangle_T)$. Related distribution functions which are relevant for the interpretation of Mössbauer and nuclear-magnetic-resonance experiments are also considered. Local spin configurations of clusters of magnetic atoms are discussed for Ising, XY, and Heisenberg systems, and it is shown that frustration effects lead to an enhancement of the variance of these distributions, as compared with corresponding distributions of a randomly diluted ferromagnet. Explicit examples are given for a model with nearest-neighbor ferromagnetic and next-nearest-neighbor antiferromagnetic exchange and random dilution with nonmagnetic atoms. Systematic series expansions for the ground state of this model are obtained (to low orders) in terms of the concentrations of both magnetic and nonmagnetic atoms. For intermediate concentrations, Monte Carlo simulations are performed for the case of the fcc lattice with classical Heisenberg spins. The results are consistent with experimental results for the $Eu_xSr_{1-x}S$ system. We also study the effect of a nonzero magnetic field and show that the magnetization process of a dilute Ising ferromagnet with competing exchange is a sort of "devil's staircase."

I. INTRODUCTION

Theoretical descriptions of static magnetic order in spin-glasses have mainly concentrated on the Edwards-Anderson order parameter q_{EA},[1,2]

$$q_{EA} = [\langle \vec{S}_i \rangle_T \cdot \langle \vec{S}_i \rangle_T]_{av} \ ; \tag{1}$$

here $\vec{S}_i$ denotes the m-component spin at lattice site i, $\langle \cdots \rangle_T$ is a thermal average for a fixed realization of disorder in the system, while finally $[\cdots]_{av}$ denotes the configurational average over this (quenched) disorder. However, increasing evidence has been presented[2–4] that the "sharp cusp" of the susceptibility χ at the freezing temperature T_f is not due to a static phase transition where q_{EA} is nonzero below T_f: rather the cusp is a dynamic phenomenon, and $q_{EA} \equiv 0$ at all nonzero temperatures for both two-dimensional[3] and three-dimensional[4] spin-glasses.

Nevertheless in spin-glasses there exists a wealth of experimental data on local magnetic order, which has an essentially static character, and can be seen both in neutron scattering experiments and in measurements utilizing "local probes" such as the Mössbauer effect, electron paramagnetic resonance (EPR), nuclear magnetic resonance (NMR), muon spin resonances (μSR), and so on.[5] These latter methods have the advantage that due to differing local environments not only average correlations but also their distributions are probed. These distributions should contain information on the "frustration" effects,[6] which are also responsible for the destruction of long-range order in spin-glasses (and hence[2] $q_{EA} \equiv 0$). Thus a study of these distributions is of interest, and hence this problem is the subject of the present paper. It is also felt that more detailed knowledge of these static correlations is needed before one can turn to a quantitatively satisfactory theory for dynamic phenomena.

The spin-spin correlation is defined by

$$g_{\vec{r}} = \langle \vec{S}_{\vec{r}_1} \cdot \vec{S}_{\vec{r}_1+\vec{r}} \rangle \ . \tag{2}$$

In inhomogeneous systems $g_{\vec{r}}$ depends on the position $\vec{r}_1$. Sampling over different $\vec{r}_1$ of the spins $\vec{S}_{\vec{r}_1}$ we generate a distribution $P(g_{\vec{r}})$ of the correlation function. This distribution is related to that of local magnetic energies $\mathcal{H}_{\vec{r}_1}$ via

$$\mathcal{H}_{\vec{r}_1} = -g\mu_B \vec{S}_{\vec{r}_1} \cdot \vec{H}_{\vec{r}_1} = -\sum_{\vec{r}} J(\vec{r}) g_{\vec{r}} \ . \tag{3}$$

The distribution of this quantity has already been studied for the case of the Edwards-Anderson bond model.[7] At $T=0$ $P(\mathcal{H})$ is the distribution of "effective fields" $H_{\vec{r}_1}$ which is discussed in the context of mean-field approaches.[8] Here we will obtain the energy distribution for a more realistic site disorder model.

The local hyperfine field B observed in resonance experiments[9] is also related to $g_{\vec{r}}$. Since usually $B(\vec{r}_1)$ has contributions from first and second neighbors only, one has

$$B(\vec{r}_1) = B_0 + f_{NN} \sum_{\vec{r}\,NN} g_{\vec{r}} + f_{NNN} \sum_{\vec{r}\,NNN} g_{\vec{r}} \ . \tag{4}$$

Thus the line shape of NMR of Mössbauer signals is related to the distributions of first- and second-neighbor spin-spin correlations. The first two moments of $P(g_{\vec{r}})$ are of interest, too. The average correlation $[g_{\vec{r}}]_{\rm av}$ is accessible via the Fourier transform of the quasielastic neutron scattering intensity. The second moment

$$g_{\rm EA}(\vec{r}) = [\langle \vec{S}_{\vec{r}_1} \cdot \vec{S}_{\vec{r}_1+\vec{r}} \rangle^2]_{\rm av} - [\langle \vec{S}_{\vec{r}_1} \cdot \vec{S}_{\vec{r}_1+\vec{r}} \rangle]^2_{\rm av} \tag{5}$$

becomes long ranged if the Edwards-Anderson order parameter in nonzero,[2]

$$\lim_{\vec{r}\to\infty} g_{\rm EA}(\vec{r}) = q^2_{\rm EA} \ . \tag{6}$$

Before we discuss the spin-spin correlations for frustrated spin-glass models we want to mention their properties for two models without frustration. First consider the Mattis model[10] of spin-glasses

$$\mathcal{H}_{\rm Mattis} = -\sum_{\langle ij \rangle} \epsilon_i \epsilon_j |J_{ij}| \vec{S}_i \cdot \vec{S}_j \ , \quad \epsilon_i = \pm 1 ({\rm random}) \ . \tag{7}$$

For constant $|J_{ij}| = J > 0$, one can "gauge away" all disorder by the transformation $\vec{S}_i = \epsilon_i \vec{\sigma}_i$. With

$$g_{\vec{r}} = \epsilon_{\vec{r}_1} \epsilon_{\vec{r}_1+\vec{r}} \langle \vec{\sigma}_{\vec{r}_1} \cdot \vec{\sigma}_{\vec{r}_1+\vec{r}} \rangle \tag{8}$$

any disorder is left in the sign of $\epsilon_{\vec{r}_1} \cdot \epsilon_{\vec{r}_1+\vec{r}} = \pm 1$. Thus $P(g_{\vec{r}})$ is a two-δ distribution.

If $|J_{ij}|$ is taken from a continuous distribution the model still has trivial ground-state properties. For $T=0$ one has the same distribution as before, namely,

$$P(g_{\vec{r}}) = \tfrac{1}{2}(1+[\epsilon]_{\rm av})\delta(g_{\vec{r}}-1) + \tfrac{1}{2}(1-[\epsilon]_{\rm av})\delta(g_{\vec{r}}+1) \ . \tag{9}$$

However, one gets nontrivial correlations at finite temperatures, and Monte Carlo simulations have shown[11] that this model has many qualitatively similar properties as the Edwards-Anderson model, although there is no frustration in the Mattis model. Secondly we consider these correlations for an "ordinary" dilution problem. Consider a ferromagnet where magnetic atoms are randomly replaced by nonmagnetic ones with probability $1-x$. These spins which belong to the same cluster are always ferromagnetically aligned, therefore one has at $T=0$ for these correlations

$$P(g_{\vec{r}}) = x\delta(g_{\vec{r}}-1) + (1-x)\delta(g_{\vec{r}}) \ . \tag{10}$$

Similarly, $P(\sum g_{\vec{r}})$ can be obtained easily as well where the sum is performed over the range of interactions. Noting that $P(\sum g_{\vec{r}})$ is nonzero only if $g_{\vec{r}}$ takes an integer value $0, 1, \ldots, z_i$, for $\vec{r}_1 + \vec{r}$ lying in the ith neighbor shell of $\vec{r}_1$, we write

$$P\left(\sum g_{\vec{r}}\right) = \sum_{n=0}^{Z_i} \binom{Z_i}{n} x^n (1-x)^{Z_i-n} \delta\left(\sum g_{\vec{r}} - n\right) \ . \tag{11}$$

From Eq. (11) it is straightforward to obtain mean and variance of the correlation $g_{\vec{r}}$ as

$$\left[\sum g_{\vec{r}}\right]_{\rm av} = \int d\left(\sum g_{\vec{r}}\right) P\left(\sum g_{\vec{r}}\right) = xZ_i \ , \tag{12}$$

$$V \equiv \left[\left(\sum g_{\vec{r}}\right)^2\right]_{\rm av} - \left(\left[\sum g_{\vec{r}}\right]_{\rm av}\right)^2 = x(1-x)Z_i \ . \tag{13}$$

Finally we note that the energy distribution is

$$P(\mathcal{H}_{\vec{r}_1}) = P\left(-\sum_{\vec{r}} J(\vec{r}) g_{\vec{r}}\right) = \sum_i \sum_{n_i=0}^{Z_i} \binom{Z_i}{n_i} x^{n_i-1} (1-x)^{Z_i-n_i} \delta\left(\mathcal{H}_{\vec{r}_1} + \sum_i n_i J_i\right) \ . \tag{14}$$

So far we have introduced the correlations of unfrustrated models. With the inclusion of competing interactions, however, the situation is much more complicated, even in the ground state. In the following section the frustration effect on local spin configuration in Ising, XY, and Heisenberg spin-glasses is discussed. In Sec. III concentration expansions and Monte Carlo results for the correlation distributions are presented. Finally, Sec. IV contains our conclusions and briefly mentions relevant experimental work[7] on the $Eu_xSr_{1-x}S$ system.

II. CONFIGURATIONS WITH NONFERROMAGNETIC SPIN ALIGNMENT IN DILUTED FERROMAGNETS WITH COMPETING INTERACTIONS

As a simple model of a system which has a (super) paramagnetic phase at very low concentrations x of magnetic atoms, a spin-glass state at intermediate and a ferromagnetic phase at high concentrations, we consider a Hamiltonian with nearest-neighbor (NN) exchange $J_1 > 0$ and next-nearest-neighbor (NNN) ex-

change $J_2 < 0$,[12]

$$\mathcal{H} = -J_1 \sum_{i,j\,\mathrm{NN}} c_i c_j \vec{S}_i \cdot \vec{S}_j + J_2 \sum_{i,j\,\mathrm{NNN}} c_i c_j \vec{S}_i \cdot \vec{S}_j \quad . \quad (15)$$

Here $c_i = 1$ if the ith lattice site is taken by a magnetic atom and zero otherwise, and hence $[c_i]_{\mathrm{av}} = x$. Both for the two-dimensional Ising case and the three-dimensional Heisenberg case the phase diagram has qualitatively the structure as shown in Fig. 1.[12] In the pure system ($x = 1$), one has a transition from a paramagnetic state to ferromagnetic one at T_c ($x = 1$) as long as $R \equiv J_2/J_1 > R_m$, while for $R < R_m$ the ordered state [which occurs for temperatures $T < T_N$ ($x = 1$)] is antiferromagnetic. Both transition temperatures T_c, T_N go to zero temperature at the multicritical point $T = 0$, $R = R_m$.[13] In the diluted case for $R < 0$ a spin-glass state occurs for concentrations $x_c' < x < x_c''$, where x_c' is the critical concentration for the transition paramagnet spin-glass in the ground state $T = 0$, and x_c'' is the critical concentration for the transition spin-glass ferromagnet. For $R \to R_m$ the critical line x_c'' [and perhaps also the line x_c' (Ref. 12)] tends to the multicritical point R_m, $T = 0$.[14] At intermediate values of R, the phase diagram in the T-x plane has then both spin-glass and ferromagnetic states, as indicated by the left of the three shaded phase diagrams in Fig. 1. An experimental example for this case[15] is provided by $Eu_xSr_{1-x}S$ (note that there $R \cong -\frac{1}{2}$, while $R_m = -1$ for the case of fcc lattice).

It has already been pointed out in Ref. 12 that the greater instability of the ferromagnetic state against dilution for $R < 0$ is due to the fact that the spins in the "infinite cluster" coupled together by exchange interactions are no longer aligned all parallel to each other, such as occurs for $R \geq 0$. In the Ising case, one can identify typical cases of spin configurations for both $x \to 0$ or 1, where spins are either aligned antiparallel or not aligned at all.[12] Here we extend these considerations to the XY and Heisenberg case, and investigate the effect of this nonferromagnetic alignment on the spin-correlation functions and their distributions.[16]

Let us start by considering the very dilute limit $x \to 0$, where the magnetic atoms occur in small clusters of monomers, dimers, trimers, etc., well separated from each other (Fig. 2). Isolated atoms do not contribute to the magnetic correlation at all, of course. For $x \to 0$ the dominating contributions to the correlations are due to pairs [Figs. 2(a) and 2(b)]. Nearest-neighbor pairs are ferromagnetically aligned, and next-nearest neighbors antiferromagnetically, irrespective of spin dimensionality. Thus the average correlation for nearest-neighbor distances will be the same for $x \to 0$ as for the ferromagnetic state, $x \to 1$, and deviations from this ferromagnetic nearest-neighbor correlation are hence expected for inter-

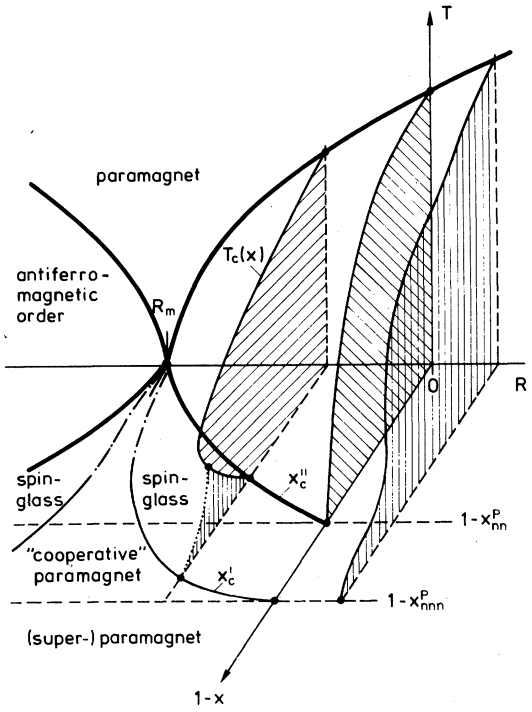

FIG. 1. Schematic phase diagram of a diluted magnet with nearest-neighbor ferromagnetic exchange J_1 and next-nearest-neighbor antiferromagnetic exchange J_2 as a function of the concentration x of magnetic sites, of temperature T and the ratio $R = J_2/J_1$. Full curves describe the second-order phase transition (dash-dotted portions are hypothetical). The dotted curve represents the "freeze-in" into a (metastable) spin-glass state.

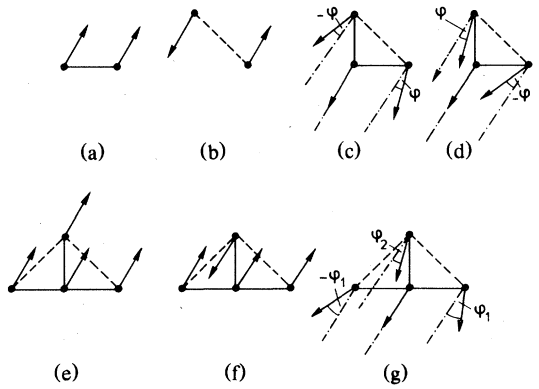

FIG. 2. Spin configurations of isolated clusters of magnetic atoms: pairs (a) and (b), triplets (c) and (d), and quadruplets (e), (f), and (g). Nearest-neighbor exchange is indicated by full and next-nearest-neighbor exchange by broken bonds. Dash-dotted lines indicate alignment direction of the corresponding spin configurations in the Ising case. For further explanations cf. text.

mediate concentrations only. The correlation of spins at next-nearest neighbor distances, on the other hand, must change from ferromagnetic (for $x \to 1$) to antiferromagnetic (for $x \to 0$).

For larger clusters less trivial possibilities occur. In Table I and Figs. 2 and 3 some simple examples are listed. In the Ising case there exists a threshold for the coupling ratio R below which the ferromagnetic alignment changes into a more complicated one as shown in Figs. 2(e) and 2(f) and 3(a), 3(b), and 3(c) for $R < -\frac{1}{2}$ and < 0, respectively. It is interesting to note that an average over the three degenerate configurations of Figs. 3(a), 3(b), and 3(c) leads to noninteger values of $g_{\frac{1}{3}}$ even in the Ising case. Here the second-neighbor correlation takes the values $\pm\frac{1}{3}$. For larger clusters more and more degenerate states and hence more and more intermediate values for the correlations (averaged over ground states of the cluster) occur. Thus the distribution function of spin correlations becomes quasicontinuous even in the Ising case, although it will have most of its weight at values ± 1 for all x.

In the XY and Heisenberg case the spins are again ferromagnetically aligned for R above a critical ratio R_c. However, R_c differs from that of the Ising model [compare Figs. 2(e) and 2(g)] and the spins gradually change their angle ϕ between each other. Apart from an overall rotation of the spins there are more degeneracies as shown in Figs. 2(c) and 2(d). In the XY model the system has the same energy for ϕ and $-\phi$. In the Heisenberg case there is an additional rotation of spin directions around the dash-dotted line. Even in the Heisenberg case the spin directions still are in a common plane. Only for four and more degrees of freedom the Heisenberg case may differ from the XY one.

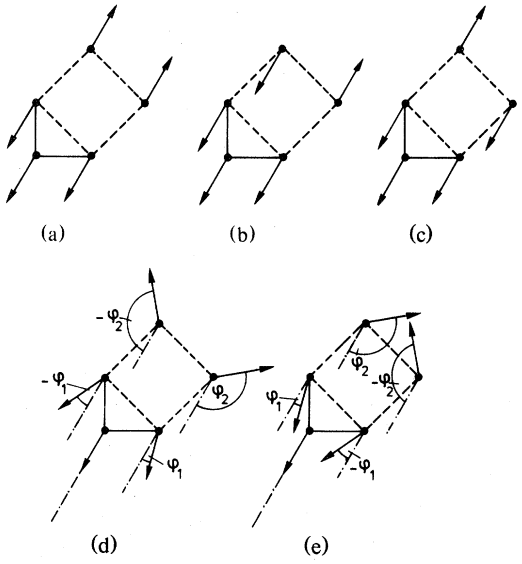

FIG. 3. Spin configuration of a certain cluster of five magnetic atoms: (a), (b), and (c) denote the three degenerate states in the Ising case, while (d) and (e) denote the two degenerate states in the XY case. For notation, cf. Fig. 2.

Next we consider the ferromagnetic limit, $x \to 1$ and $R > -\frac{1}{2}$. With probabilities of order $(1-x)^k$ we find clusters of k nonmagnetic atoms which are either

TABLE I. For coupling ratio $R = J_2/J_1 < R_c$ the XY or Heisenberg spins of configurations Figs. 2, 3, and 4 have a noncollinear ground state. Critical ratios R_c, the energies of the noncollinear spins U_c, and their angles ϕ_i are given for some simple examples.

Fig.	R_c	U_c/J_1	ϕ_i
2(c), 2(d)	$-\frac{1}{2}$	$\left(R+\frac{1}{2R}\right)\Big/3$	$\cos\phi = -1/2R$
2(g)	$-1 < R < -\frac{1}{3}$	$-(5R^2+1)/2R$	$\cos\phi_1 = -(1+3R^2)/4R$
3(d), 3(e)	0		$\phi_2 = \frac{\pi+\phi_1}{3}$, $\phi_1 = \pm\frac{\sqrt{3}}{2}R + O(R^2)$
4(a), 4(b)	$-\frac{2}{5} - \frac{1}{5}H/J_1$	$\frac{11R}{2}+6+\frac{2}{R}(H=0)$	$\cos\phi = \left(1+\frac{3R}{2}+\frac{1}{2}\frac{H}{J_1}\right)\Big/R$
4(c)	$-\frac{1}{3}(1+H/J_1)$	$\frac{2}{R}+4+6R\,(H=0)$	$\cos\phi = \left(1+R+\frac{1}{2}\frac{H}{J_1}\right)\Big/(2R)$

nearest or next-nearest neighbors on the lattice. Figure 4 shows some examples in low orders in the variable $1-x$. In the Ising case the first configuration containing antiparallel spins occurs in order $(1-x)^3$, Fig. 4(e), while for the XY and Heisenberg model deviations from ferromagnetic alignment occur in order $(1-x)^2$, Figs. 4(a) and 4(b). In Table I angles, thresholds, and energies are given for the cases shown in Fig. 4. The energy can still be lowered to some extent by relaxing the ferromagnetic alignment of the surrounding spins. The deviation $\Delta\phi$ from the ferromagnetic axis decays with some inverse power of the distance $|\vec{r}|$ to the defect.[16]

In the XY model one again has the degeneracy $\pm\phi_i$ of the canted spins, while in the Heisenberg case against rotation around the ferromagnetic axis is possible. These additional degrees of freedom interact via the deviations $\Delta\phi(\vec{r})$ of the spins between the defects, therefore they may freeze into a spin-glass phase at low temperatures.[16] In Table I and Fig. 4, an external magnetic field has been included, too. An important observation is that the angle ϕ goes to zero continuously if H is increased. In the Ising case, on the other hand, antiparallel spins do not change their orientation in weak fields, until a critical field H_c is reached [in the case of Fig. 4(e) we have $H_c/J_1 = -1-4R$, for $R < R_c = -\frac{1}{4}$]. At this critical field, the orientation of an antiparallel spin jumps discontinuously from -1 to $+1$.

As a result, we predict for the magnetization process of a diluted Ising ferromagnet with competing interactions a sequence of magnetization jumps, occurring at critical fields where clusters of antiparallel spins start to become parallel oriented. Thus, consider the general case where a cluster of l spins, which is coupled by m nearest-neighbors J_1 and n next-nearest bonds J_2 to its (ferromagnetic) environment. This cluster will be overturned when the energy difference $\Delta U = mJ_1 + nJ_2 + lH = 0$, i.e., critical field is

$$H_c/J_1 = -m/l - (n/l)R \quad . \tag{16}$$

While for small l the geometrical possibilities allow only a few choices of m and n, for large l, m and n will take on a variety of possible values, corresponding to the various configurations of empty sites at the surface of this cluster. Since for large enough compact clusters both m/l and n/l may be arbitrarily small, the magnetization process is a sort of "devil's staircase" of singularities. Note that the magnitude of the magnetization jump decreases rapidly with increasing cluster size, and therefore the behavior will be qualitatively as shown in Fig. 5. In contrast, for

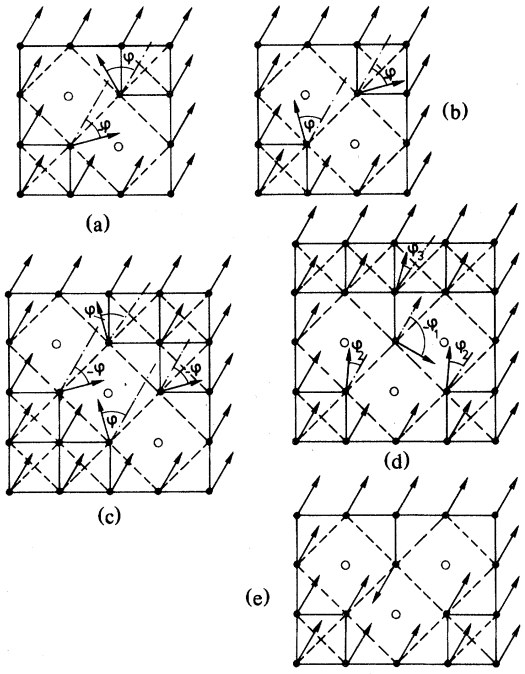

FIG. 4. Spin configurations near clusters of nonmagnetic atoms (indicated as empty circles) in the XY case [(a)–(d)] and Ising case [(e)]. For notation, cf. Fig. 2, for further explanations cf. text.

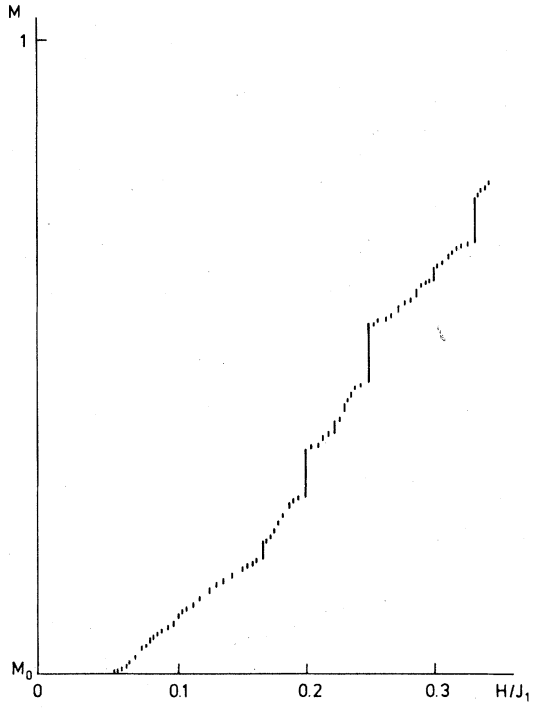

FIG. 5. Qualitative magnetization process of a diluted Ising system with $R = -\frac{1}{3}$ at a concentration x in the range $x_c'' < x < 1$. Magnetization jumps occur for $H_c/J_1 = (n-3m)/3l$, where n, m, and l are integers (cf. text).

XY and Heisenberg systems the magnetization process is predicted to be perfectly smooth. Computer simulations for a diluted fcc classical Heisenberg model with $R=-\frac{1}{2}$ confirm this prediction (Fig. 12). These calculations are in qualitative agreement with corresponding experimental data for the $Eu_xSr_{1-x}S$ dilution system.[17]

III. DISTRIBUTION FUNCTIONS FOR MAGNETIC CORRELATIONS: NUMERICAL RESULTS

A. Exact concentration expansions for the square Ising model

In order to derive a systematic expansion of the distributions $P(\sum g_{\vec{r}})$, $P(\mathcal{H}_{\vec{r}_1})$ in powers of the concentration x, on which we concentrate our interest in the following, one has to compute the quantities $\sum g_{\vec{r}}$, $\mathcal{H}_{\vec{r}_1}$ for each possible site of a cluster (such as shown in Figs. 2 and 3, etc.), and weigh the resulting contributions with the corresponding statistical factor appropriate for that particular cluster. Finally the result is summed over all possible clusters up to some given maximal cluster size, and the resulting expression is then expanded in powers of x. Computing the statistical weights we assume perfectly random mixing (although the procedure can in principle be extended to include "chemical clustering" effects or any prescribed short-range order in the occupation probabilities of magnetic atoms). Experience with similar expansions for other quantities[12] has shown that in higher order the coefficients typically behave rather irregularly reflecting singularities of the same nature as those in Fig. 5. Thus we restrict ourselves to low orders of the expansion here, appropriate for considering the behavior near $x\to 0$ and 1 (for the expansion in the concentration of "holes" with concentration $y=1-x$).

Let us consider the conditional probabilites for the square lattice Ising system with $-0.5<R<0$ up to order x^4 (clusters of one central occupied spin and between 0 and 4 first or second neighbors). In this order of the expansion no antiparallel nearest neighbors occur; thus we have as in ordinary dilution [Eqs. (11) and (12) with $Z_i=4$ here]

$$\left[\sum g_{\vec{r}_{\mathrm{NN}}}\right]_{\mathrm{av}}=4x,\quad V_{\mathrm{NN}}=4x(1-x)\ . \tag{17}$$

For the distribution functions of the second-neighbor correlation, the situation is different, however. Clusters with free second neighbors and the central spin give integer values for $\sum_{\mathrm{NNN}} g_{\vec{r}}$ between -4 and -1. If the second neighbors are connected by nearest neighbors as in Figs. 2(c) and 2(e), $\sum_{\mathrm{NNN}} g_{\vec{r}}$ has the values 1 and 2 . Due to degeneracies as in Figs. 3(a)–3(c) the second neighbor correlation can also take rational numbers. For instance the values $\pm\frac{2}{3}$ occur with probability $8x^4$. One obtains for the average value and the variance of the next-nearest-neighbor correlation

$$\left[\sum g_{\vec{r}\,\mathrm{NNN}}\right]_{\mathrm{av}}=4x+16x^2-8x^3+16x^4\ ,$$

$$V_{\mathrm{NNN}}=4x(1-x)+64x^3-176x^4\ . \tag{18}$$

Thus the concentration dependence of this correlation differs from the ordinary dilution problem already in low order and the variance is enhanced.

The local energy is given by the spin correlations

$$\mathcal{H}=-\frac{J_1}{2}\sum_{\mathrm{NN}} g_{\vec{r}}-\frac{J_2}{2}\sum_{\mathrm{NNN}} g_{\vec{r}}\ . \tag{19}$$

The corresponding equation also holds for the conditional averages. However, the variance is given by

$$V_H=[(\mathcal{H}-[\mathcal{H}]_{\mathrm{av}})^2]_{\mathrm{av}}=J_1^2V_{\mathrm{NN}}+J_2^2V_{\mathrm{NNN}}+2J_1J_2V\ , \tag{20a}$$

$$V=\left[\left(\sum_{\mathrm{NN}} g_{\vec{r}}\right)\left(\sum_{\mathrm{NNN}} g_{\vec{r}}\right)\right]_{\mathrm{av}}-\left[\sum_{\mathrm{NN}} g_{\vec{r}}\right]_{\mathrm{av}}\left[\sum_{\mathrm{NNN}} g_{\vec{r}}\right]_{\mathrm{av}}\ . \tag{20b}$$

Since J_1J_2 is negative the correlation between first and second neighbors V reduces the variance of the energy. From Eqs. (17) and (20) we obtain

$$[\mathcal{H}]_{\mathrm{av}}=-2x(J_1-J_2)-4J_2(2x^2-x^3+2x^4)\ , \tag{21a}$$

$$V_H=x(1-x)(J_1^2+J_2^2)+4J_2^2(4x^3-11x^4)+8J_1J_2(x^2-2x^3+x^4)\ . \tag{21b}$$

Since to the order of our expansion there are no "frustrated" nearest-neighbor bonds the corrections to the leading order in Eq. (21a) involve J_2 only. Note that the variance $V_{\mathcal{H}}$ is *reduced* as compared to the variance of the pure dilution problem [$V_{\mathcal{H}}=(J_1^2+J_2^2)x(1-x)$ then], which is an unexpected result. This reduction of the variance is due to the strong correlation between local disorder and local spin arrangement, due to energy minimization.

Next the expansions of the corresponding quantities in powers of the concentration y of nonmagnetic atoms are considered. For $-0.5<R<-0.25$ and up to order y^3, only the configurations of Fig. 4(e) are responsible for different correlations as compared to ordinary dilution. From Fig. 4(e) we see that both first- and second-neighbor correlations are changed, and we obtain

$$\left[\sum_{\mathrm{NN}} g_{\vec{r}}\right]_{\mathrm{av}}=4x-16y^3\ , \tag{22a}$$

$$V_{\mathrm{NN}}=4x(1-x)+80y^3\ , \tag{22b}$$

and

$$\left[\sum_{\text{NNN}} g_{\vec{r}}\right]_{\text{av}} = 4x - 64y^3 \ , \tag{23a}$$

$$V_{\text{NNN}} = 4y(1-y) + 320y^3 \ . \tag{23b}$$

Again the distribution of the local energy can be obtained from the distributions of correlations by Eqs. (19) and (20), one obtains

$$[\mathfrak{K}]_{\text{av}} = -2x(J_1 - J_2) + 8y^3(J_1 + 4J_2) \ , \tag{24a}$$

$$V_H = y(1-y)(J_1^2 - J_2^2) + 4y^3(5J_1^2 + 20J_2^2 + 28J_1J_2) \ . \tag{24b}$$

Again the variances of the individual correlations are enhanced while the variance of the local energy distribution is reduced as compared to an ordinary dilution problem. For $R < -\frac{1}{4}$ the configuration of Fig. 4(e) is responsible for the y^3 correction to the ordinary dilution problem. It is interesting that at $R = -\frac{1}{4}$ the energy (24a) is continuous as a function of R whereas the variance has a discontinuous jump.

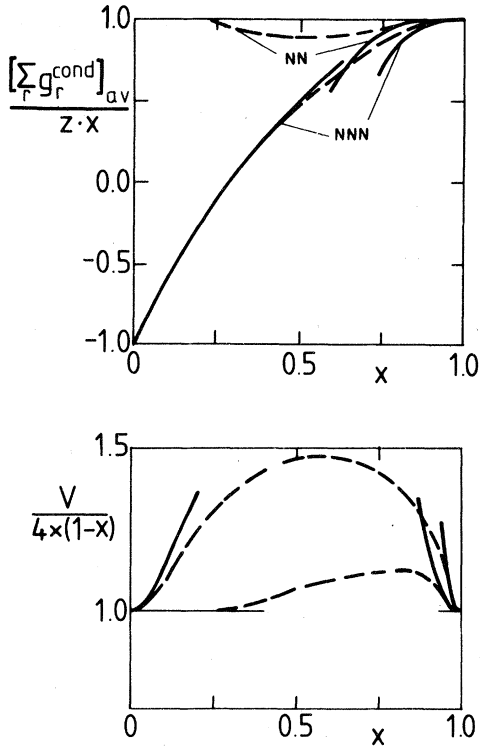

FIG. 6. Normalized conditional correlation between nearest-neighbor (NN) and next-nearest-neighbor (NNN) shells on the Ising square lattice with $J_2 < -J_1/4$ (upper part) and associated variances (lower part). Full curves represent series expansions, while broken curves indicate a qualitative interpolation.

Thus when crossing $R = -\frac{1}{4}$ from above degenerate spins are flipped without cost of energy. However, these spin flips increase the fluctuations of the surrounding local fields.

On the basis of these expansions one expects a behavior as shown in Fig. 6. Of course, a quantitative estimate of these quantities is not possible with these very short series. Even if longer series were available we would expect them to be valid only for $x < x_c'$ (x expansion) or $x > x_c''$ (y expansion), respectively: at the phase boundaries x_c', x_c'' (weak) singularities are expected for all quantities under consideration.

B. Monte Carlo calculations for the face-centered-cubic classical Heisenberg model

Being interested in the distribution of spin-spin correlations at arbitrary concentration, it is convenient to apply Monte Carlo methods.[18] We again study the model treated in Ref. 12 because it can be compared to data on $Eu_xSr_{1-x}S$.[7,15] Typically a system of 4000 sites with periodic boundary conditions is simulated.

Figure 7 shows the distribution functions of individual spin correlations $P(\langle \vec{S}_i \cdot \vec{S}_j \rangle_T)$ at a concentration deeply within the spin-glass phase. It is seen that most nearest-neighbor pairs are ferromagnetically aligned, at least to some extent. On the other hand, for next-nearest neighbors antiferromagnetic alignment is about as likely as a ferromagnetic one, and there is also considerable weight for pairs of spins

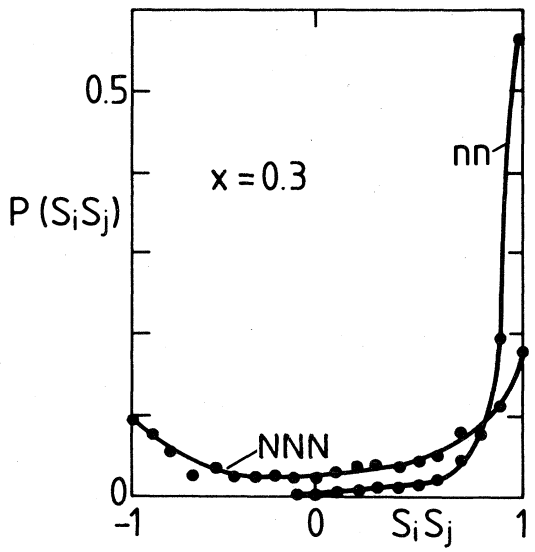

FIG. 7. Distributions $P(\langle \vec{S}_i \cdot \vec{S}_j \rangle_T)$ for nearest-neighbor (NN) and next-nearest-neighbor (NNN) sites of a classical fcc Heisenberg magnet with $J_2 = -J_1/2$ at $x = 0.3$, $T = 0$.

which are nearly orthogonal to each other.

Figure 8 shows the distribution of $P(\sum_{\vec{r}} g_{\vec{r}})$ for nearest-neighbor distances at several concentrations. In order to compare with the distribution in the ordinary dilution case, Eq. (10), for which $\sum_{\vec{r}} g_{\vec{r}}$ can take integers only, $P(\sum_{\vec{r}} g_{\vec{r}})$ was recorded as a histogram with integer stepwidth. It is seen that the actual distribution is not very different from this distribution occurring in the ordinary dilution problem. The situation is different for next-nearest-neighbor distances, however (Fig. 9). In this case, Eq. (10) would be a bad approximation. This result is particularly important for the $Eu_xSr_{1-x}S$ system, where it is believed that the next-nearest-neighbor correlations dominate in the transferred hyperfine fields.[9] Finally, Fig. 10 presents our results for the distribution of the local energy of magnetic sites, which can also be interpreted (at $T=0$) as the distribution of local effective magnetic fields H_{eff}, as noted above. Note that there is (almost) no weight near $H_{\text{eff}}=0$ for this spin-glass model.

The results of our calculations are then summarized in Fig. 11. It is seen that the mean nearest-neighbor correlation stays nearly perfectly ferromagnetic for all concentrations, while the next-nearest-neighbor correlation changes from ferromagnetic (for $x \to 1$) to antiferromagnetic (for $x \to 0$), the behavior

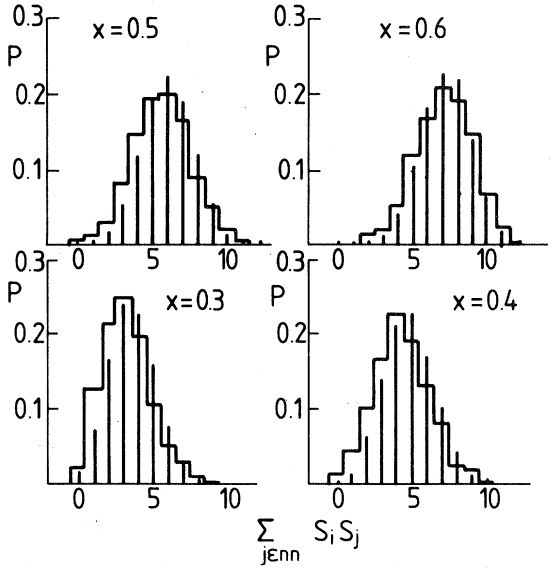

FIG. 8. Distribution $P(\sum_{\vec{r}} g_{\vec{r}})$ for the nearest-neighbor shell of a classical fcc Heisenberg magnet with $J_2=-J_1/2$ and $T=0$ at various x. The number N of sites occupied by magnetic atoms in the lattice sites also indicated. Histogram denotes recorded distribution while straight lines represent Eq. (10).

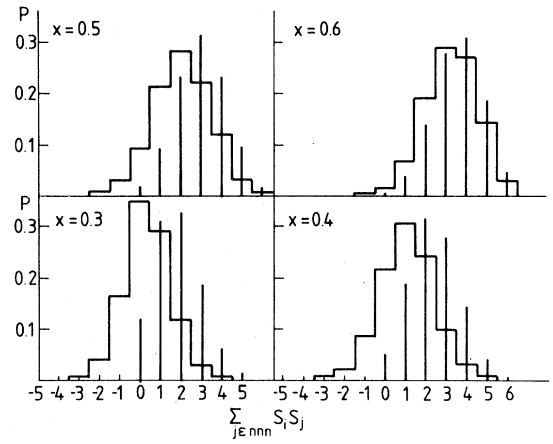

FIG. 9. Same as Fig. 8 but for the next-nearest-neighbor shell.

near $x=0$ being given by

$$\left[\left\langle S_0 \cdot S_{r_{\text{NNN}}}\right\rangle\right]_{\text{av}} \Big/ x^2 = -1 + 8x + O(x^2) \ .$$

The behavior of $[\sum_{\vec{r}} g_{\vec{r}}]_{\text{av}}$ is similar. We note that the average energy behaves as

$$[\langle \mathcal{H} \rangle]_{\text{av}} / [-(6J_1+3J_2)x^2] \to 1$$

for $x \to 1$, while

$$\frac{[\langle \mathcal{H} \rangle]_{\text{av}}}{[-(6J_1+3J_2)x^2]} \to \frac{[(6J_1+3|J_2|)-24x|J_2|]}{(6J_1+3J_2)}$$

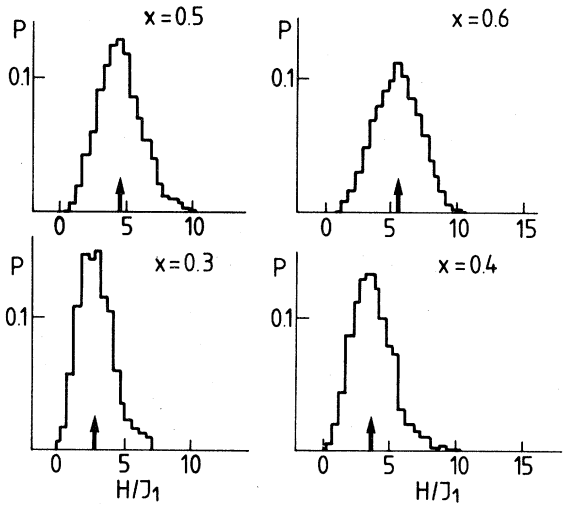

FIG. 10. Distribution of local effective magnetic fields for a classical fcc Heisenberg magnet with $J_2=-J_1/2$ at $T=0$ for various x.

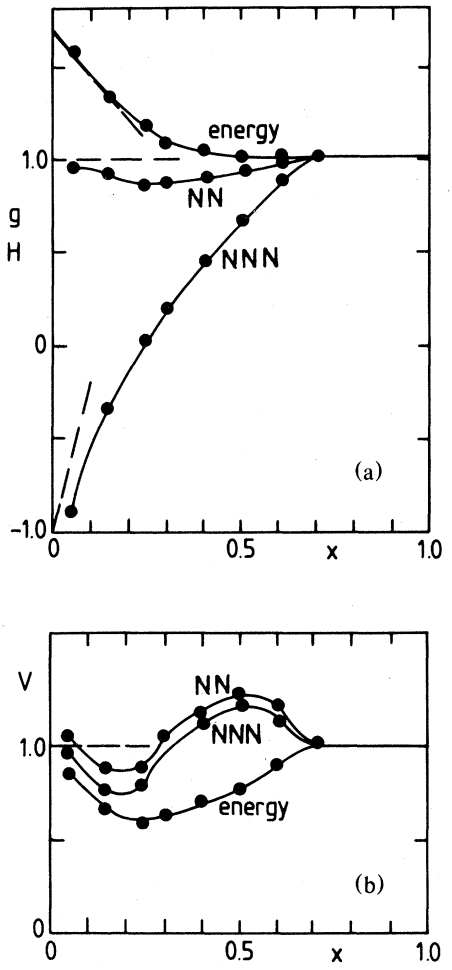

FIG. 11. Concentration dependence of individual correlations g: $[\sum_{NN} g_{\vec{r}}]_{av}/12x$, $[\sum_{NNN} g_{\vec{r}}]_{av}/6x$, and the normalized energy $H=[\mathcal{H}]_{av}/(6J_1x^2+3J_2x^2)$ (a), and of the associated variances V: $V_{NN}/[12x(1-x)]$, $V_{NNN}/[6x(1-x)]$, and $V_{\mathcal{H}}/[(12J_1^2+6J_2^2)x(1-x)]$ (b). Dashed straight lines indicate asymptotic behavior for small x.

for $x \to 0$: while *all* antiferromagnetic bonds are unsatisfactory ("frustrated") in the ferromagnetic state for $x \to 1$, there are no frustrated bonds for $x \to 0$. With respect to the variances, we note as in the Ising case that the variances of $\sum_{\vec{r}} g_{\vec{r}}$ are enhanced in comparison with an ordinary dilution problem [Eq. (10)], while the variance of the energy distribution gets reduced for intermediate concentrations.

IV. CONCLUSIONS

In this paper distribution functions of magnetic short-range order in magnets with quenched disorder were introduced, and their ground-state properties discussed. While these distributions can be obtained rather trivially for Mattis spin-glasses, dilution problems with noncompeting magnetic interactions, etc., diluted systems with competing interactions (which show nontrivial spin-glass behavior) are much more complicated. We proceeded by first analyzing the spin configurations for Ising, XY, and Heisenberg spins, and then identified the behavior of the distribution functions by exact concentration series expansions in the Ising case and by Monte Carlo computer simulations in the Heisenberg case. Our results show, at least for the model with ferromagnetic nearest- and antiferromagnetic next-nearest-neighbor exchange which is realistic for $Eu_xSr_{1-x}S$, that one can have a pronounced ferromagnetic short-range correlation throughout the spin-glass phase: it is only the ferromagnetic *long*-range order which is lost in the spin-glass phase, but locally still most of the spins are oriented nearly parallel to each other. The orientation of this local ferromagnetic order changes in the system gradually but irregularly, due to the random distribution of the configurations of nonmagnetic atoms. Of course, if an antiferromagnetic with competing interactions would be diluted rather than a ferromagnet, we expect local antiferromagnetic order instead. In fact, we expect similar local order effects in other spin-glasses such as nonmagnetic metals diluted with magnetic ions, too: but since longer-range interactions (such as the Ruderman-Kittel exchange) are cumbersome to treat by either the concentration expansion method or the Monte Carlo simulation method, we have not attempted any quantitative analysis here. We feel, however, that for a more complete understanding of spin-glass systems the analysis of such short-range-order effects will be indispensable.

As mentioned above, the present calculations have

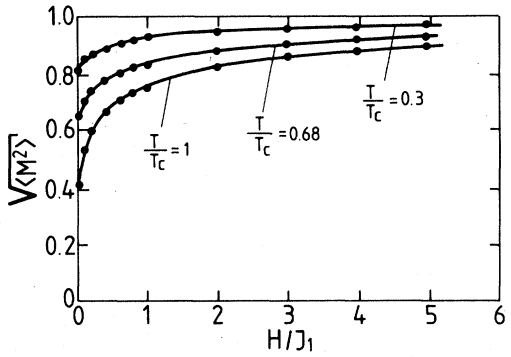

FIG. 12. Monte Carlo results for the root-mean-square magnetization as function of magnetic field of a fcc classical Heisenberg system at composition $x=0.595$, for a lattice of 4×10^3 sites and periodic boundary conditions. Note that the estimate for the critical temperature of ferromagnetic order in this case is $k_B T_c/J_1 \cong 0.95$.

immediate applications to $Eu_xSr_{1-x}S$. Thus it is gratifying that both the variation of the magnetization with an applied magnetic field (Fig. 12) and of the quantity $[\sum g_{\vec{r}}]_{av}$, which is related to the hyperfine field measured in resonance experiments, are in reasonable accord with observation. But a more quantitative analysis of the data yielding information on the full distributions would be desirable. It would also be interesting to find an experimental realization of a dilute Ising system with competing interactions: its magnetization process would be a sort of "devil's staircase" (Fig. 5). Thus we hope that the present work will stimulate further experimental efforts on spin-glasses.

[1]S. F. Edwards and P. W. Anderson, J. Phys. F 5, 965 (1975).

[2]For a recent review of theoretical work, see K. Binder, in *Fundamental Problems in Statistical Mechanics V,* edited by E. G. D. Cohen (in press).

[3]I. Morgenstern and K. Binder, Phys. Rev. Lett. 43, 1615 (1979); Phys. Rev. B 22, 288 (1980).

[4]I. Morgenstern and K. Binder, Z. Phys. B 39, 227 (1980).

[5]For recent reviews of experimental work on spin-glasses, see J. A. Mydosh, in *Amorphous Magnetism II,* edited by R. A. Levy and S. Hasegawa (Plenum, New York, 1977); P. A. Beck, Prog. Mater. Sci. 23, 1 (1978); and A. P. Murani, J. Phys. (Paris) 39, C6-1517 (1978).

[6]G. Toulouse, Commun. Phys. 2, 115 (1977).

[7]See, e.g., K. Binder, J. Phys. (Paris) 39, C6-1527 (1978), and references therein.

[8]M. W. Klein and R. Brout, Phys. Rev. 132, 2412 (1963); M. W. Klein, Phys. Rev. B 14, 5008 (1976).

[9]H. Lütgemeier, Ch. Sauer, and W. Zinn, in *Nuclear and Electron Resonance Spectroscopies Applied to Materials Science,* edited by Kaufmann and Shenoy (North-Holland, Amsterdam, 1981), p. 467.

[10]D. C. Mattis, Phys. Lett. 56A, 421 (1976).

[11]C. Dasgupta, S.-K. Ma, and C.-K. Hu, Phys. Rev. B 20, 3837 (1979).

[12]K. Binder, W. Kinzel, and D. Stauffer, Z. Phys. B 36, 161 (1979).

[13]In the Heisenberg this description applies to the classical limit, spin quantum number $S \to \infty$, only. For finite S there is a finite (albeit small) range of values R around R_m where the system stays paramagnetic down to zero temperature, see H. P. Bader and R. Schilling, Phys. Rev. B 19, 3556 (1979).

[14]For an experimental example of the situation where very small dilution already destroys magnetic order see K. Westerhold and H. Bach (unpublished).

[15]For a recent review, see H. Maletta, J. Phys (Paris) 41, C5-115 (1980).

[16]For a discussion of nonparallel spin alignment in XY and Heisenberg spin-glasses with simpler $\pm J$-bond disorder, see J. Villian, J. Phys. C 10, 4793 (1977); 11, 745 (1978).

[17]U. Köbler (unpublished data).

[18]*Monte Carlo Methods in Statistical Physics,* edited by K. Binder (Springer, Berlin, 1979).